Byoungsok Jung[1]
Rajiv Bharadwaj[2]
Juan G. Santiago[1]

[1]Department of Mechanical Engineering
[2]Department of Chemical Engineering, Stanford University, Stanford, CA, USA

Thousandfold signal increase using field-amplified sample stacking for on-chip electrophoresis

Field-amplified sample stacking (FASS) leverages conductivity gradients between a volume of injected sample and the background buffer to increase sample concentration. A major challenge in applying FASS to on-chip assays is the initial setup of high-conductivity gradient boundaries in the region of the injected sample volume. We have designed, fabricated, and characterized a novel FASS-capillary electrophoresis (CE) chip design that uses a photoinitiated porous polymer structure to facilitate sample injection and flow control for high-gradient FASS. This polymer structure provides a region of high flow resistance that allows the electromigration of sample ions. We have demonstrated an electropherogram signal increase by a factor of 1100 in electrophoretic separations of fluorescein and Bodipy with, respectively, 2 μM and 1 μM initial concentrations.

Keywords: Capillary electrophoresis / Field-amplified sample stacking / Microfluidic chip / Miniaturization / Photoinitiated polymerization DOI 10.1002/elps.200305611

1 Introduction

On-chip electrophoresis devices offer reduced sample volumes, rapid analysis time, and ease of automation [1]. One drawback of microchannels is that the depth dimensions of etched channels (typically 10–20 μm deep) provide a short line-of-sight-integration length for optical detectors, and this adversely affects their limit of detection. One way of improving limit of detection is to integrate an on-line preconcentration process for sample analytes. Sample preconcentration offers higher sensitivity assays, robust electrokinetic injection schemes, and the use of detection modes less sensitive than fluorescence, such as electrochemical detection [2]. Field-amplified sample stacking (FASS) was first discussed by Mikkers *et al.* [3] for free-standing capillaries, and first implemented to a microchip by Jacobson and Ramsey [4]. FASS is one of the most important preconcentration methods for on-chip electrophoresis as it is easily implemented into on-chip capillary zone electrophoresis (CZE) systems and provides a single-step method of achieving high sensitivity [5, 6]. Prior to the current work, on-chip FASS as a stand-alone method has been limited to less than 10^2-fold increases in signal strength [7, 8].

Correspondence: Byoungsok Jung, 488 Escondido Mall, Bldg 500 Room 500X1, Stanford, CA 94305, USA
E-mail: bsjung@stanford.edu
Fax: +650-723-7657

Abbreviations: AIBN, azobisisobutyronitrile; **EDMA**, ethylene dimethacrylate; **FASS**, field-amplified sample stacking; **GMA**, glycidyl methacrylate

In conventional on-chip FASS systems, a sample analyte is dissolved in a solution of low ionic conductivity, and a small volume of this solution is introduced into the microchannel system using various electrokinetic- or pressure-injection methods. The key steps in the process are depicted schematically in Fig. 1. A background buffer in the system has a relatively high ionic conductivity. Sample ions drift within the high field (high electrophoretic velocity) sample region, pass through the conductivity interface region, and stack on the far side of the interface (front interface for positive ions and rear for negative ions). The key to achieving ultrahigh signal increases ($>$ 1000) using FASS lies in reproducibly achieving very high concentration-gradient regions in an on-chip system. Two challenges to this are the dispersion caused by nonuniform wall mobilities in FASS devices with finite electroosmotic flow (EOF) [9], and the fact that electrokinetic flows with high-conductivity gradients are highly unstable [10]. Chen *et al.* [10] showed that these instabilities lead to unsteady flow conditions that greatly disturb the desired conductivity gradients. Burgi and Chien [11] studied sample dispersion dynamics and electrophoretic peak broadening caused by EOF mobility mismatch in FASS. Yang and Chien [8] discuss the difficulties in combined pressure- and electrokinetic control of sample injection in a variety of chip designs, and demonstrated a signal increase factor of 100. Lichetenberg *et al.* [7] also discuss the issues associated with electrokinetic injections of heterogeneous buffer samples. In an effort to cope with these issues, the latter group opted for a complex, six-channel intersection geometry, and demonstrated a maximum signal increase of 65.

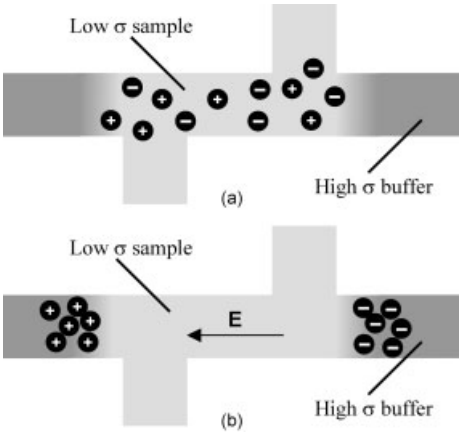

Figure 1. Schematic of on-chip FASS in the absence of EOF. Gray shading is used to show conductivity field, with lighter shading corresponding to low-conductivity buffer. Only sample ions (typically present in lowest concentration) are shown. (a) Anionic and cationic sample ions are introduced into the horizontal separation channel within a region of low ionic conductivity. (b) On application of an electric field along the separation channel, sample ions exit the low conductivity/high electric field region and enter the low electric field region. Sample concentration increases as sample ions cross the interface between the high- and low-conductivity buffers. Cations electromigrate in the direction of electric field and stack at the interface on the cathode side, while anions stack at the anodic interface.

In this paper, we describe a novel porous-polymer-plug CE chip design and an associated FASS process that can be used to achieve more than 1000-fold increases in electropherogram signals. The system achieves this with a very simple pressure flow control scheme that uses a single pressure-driven loading step for buffer, followed by a single pressure-driven loading step for sample ions. These loading steps are then followed by standard high-voltage electrokinetic injection process.

2 Materials and methods

2.1 Materials

Ethylene dimethacrylate (EDMA; Sartomer, Exton, PA, USA), glycidyl methacrylate (GMA; Sartomer), and azobisisobutyronitrile (AIBN; Aldrich, Milwaukee, WI, USA) were obtained from Prof. F. Svec (University of California, Berkeley, CA, USA). A 5 mM HEPES (Sigma, St. Louis, MO, USA) buffer solution with a pH of 7.0 was used with a 0.4 wt% methylcellulose (Aldrich) solute to suppress EOF [12]. A high-conductivity buffer (77.6 mS/cm) was prepared by dissolving a requisite amount of NaCl salt (J.T. Baker, Phillipsburg, NJ, USA) to HEPES buffer. Our sample solute consists of an aqueous solution of 1 μM Bodipy (Molecular Probes, Eugene, OR, USA) and 2 μM fluorescein (J.T. Baker). All sample and buffer solutions were filtered through 0.2 μm syringe filters before use. The conductivity of buffer and sample solution were measured using a conductivity meter (Jenco Instruments, San Diego, CA, USA).

2.2 Instrumentation

A schematic of the FASS CE visualization system is shown in Fig. 2. The system consists of an intensified CCD camera (Roper Scientific, IPentaMAX, Trenton, NJ, USA), an inverted epifluorescent microscope (IX70, Olympus, Melville, NY, USA) fitted with a 10× objective (numerical aperture (N.A.) of 0.3, Olympus), a high-voltage power supply (Micralyne, Alberta, Canada), and a syringe pump (Pump 33, Harvard Apparatus, South Natick, MA, USA). An XF100–3 filter cube (Omega Optical, Brattleboro, VT, USA) with peak excitation and emission wavelength ranges of 450–500 nm and 500–575 nm, respectively, was used.

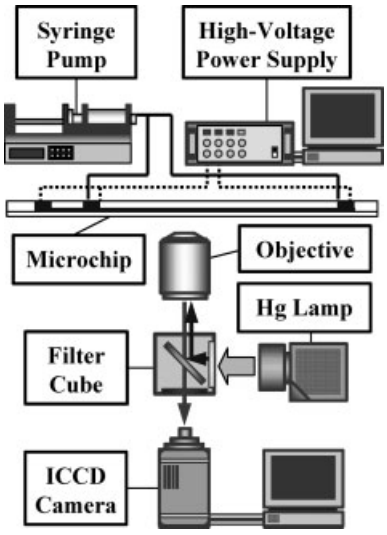

Figure 2. Schematic of FASS-/on-chip electrophoresis experiment setup showing imaging equipment, syringe pump used for pressure-injection control, and multi-port high-voltage power supply. Various pressure/flow and electrical connections to the chip are also shown as solid and dashed lines, respectively.

2.3 Porous structure fabrication and pore characterization

The glass microchannel used had a double-T injection geometry and is available commercially from Micralyne. The channel widths in this device are 50 μm and channel

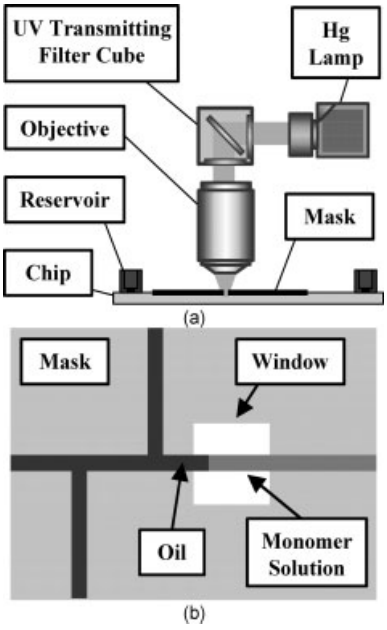

Figure 3. Schematic of the experimental setup used of fabrication of a porous polymer plug in a microchannel. (a) Side view showing UV light emitted from a mercury arc lamp and directed through a microscope objective onto the chip. (b) Top view of chip and photomask showing the position of the transmitting window in the shadow mask. The upstream (left-most) edge of the porous plug is defined using an oil-water interface (regions filled with oil are shown in black) and the downstream edge of the plug is defined by the right edge of the mask window.

depth is everywhere a maximum 20 μm. The porous polymer plug was fabricated using the photoinitiated polymerization process described by Yu *et al.* [13]. The setup and polymerization equipment are shown schematically in Fig. 3. The monomer (0.96 g EDMA, 1.421 g GMA), porogenic solvent (50/50 wt% methanol/3.6 g ethanol), and photoinitiator (24 mg AIBN) were mixed and purged with nitrogen for 10 min before use. The microchannel device was rinsed with 0.1 M NaOH for 10 min, followed by deionized water for 30 min using a syringe pump. The upstream interface location of the porous structure was photodefined by positioning an immiscible-interface (of oil and the aqueous polymerization solution) near the injection region of the chip and the downstream, less critical interface was defined using a printed ink-on-mylar film shadow mask as shown schematically in Fig. 3b. Broadband light from a mercury arc lamp was focused for 4 h on the plane of microchannel using an epifluorescent microscope. The microchannel with the *in situ* polymerized plug structure is shown in Fig. 4. After polymerization was complete, the remaining monomer solution was removed from the system by rinsing the microchannel with methanol for 2 h and then deionized water for 3 h using a syringe pump. The pore diameter distribution of our porous polymer structures was analyzed by polymerizing monoliths off-chip. A small glass chamber was filled with the same monomer solution, and then exposed to similar polymerization conditions. After polymerization, the monoliths were removed from the glass chamber, washed with methanol and dried. Figure 5 shows a pore diameter distribution measurement obtained using a mercury intrusion porosimeter (Tripp *et al.*, unpublished). The median pore diameter is about 4.6 μm. These measurements are consistent with the work of Yu *et al.* [13].

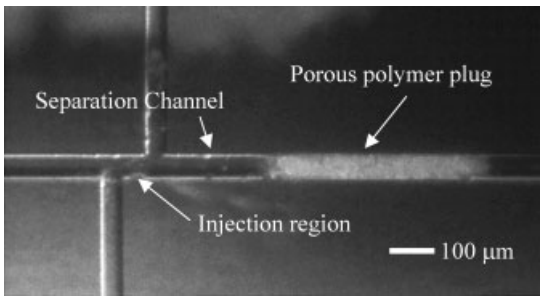

Figure 4. Reflective mode (elastic light scatter) microscopy image of porous polymer plug in a glass microchannel with a double-T injection geometry. The microchannels are 50 μm wide at the top, 20 μm deep, and have a D-shape characteristic of wet etching of glass. The polymer plug is 500 μm long and the leading edge is positioned 310 μm from the center of the injection region between the two T-shaped intersections.

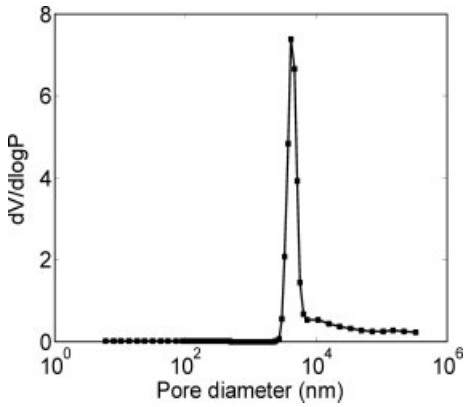

Figure 5. Pore size distribution of the porous polymer measured using a mercury intrusion porosimeter (Autopore III 9400, Norcross, GA, USA). Pore diameter density is quantified as the derivative of specific volume in mL/g with respect to the (base 10) logarithm of intrusion pressure in Pa. The median pore diameter for the polymer material used here was 4.6 μm. The full-width at half-maximum of the peak is 1.6 μm.

2.4 FASS-CE protocol

The on-chip integrated polymer structure shown in Fig. 4 provides a region of high resistance to pressure-driven flow that still allows electrophoretic migration to take place. This allows for a pressure-injection scheme that has two advantages: First, the scheme enables the device to achieve a high conductivity gradient within the separation channel in a chip with suppressed electroosmotic mobility (in this case, using 0.4% methylcellulose). Suppression of EOF minimizes sample dispersion during the simultaneous FASS-CE electrophoresis process. Second, the pressure-injection scheme allows us to avoid electrokinetic instabilities. Electrokinetic (EK) flow instabilities occur in electrically driven flows of electrolytes with high ionic conductivity gradients [10]. These instabilities can cause excessive dispersion of the buffer-buffer interface and hence limit the performance of FASS with high stacking ratios. In the sample injection process described in this section, we avoid EK instabilities by establishing the initial conductivity gradients within the separation channel using pressure-driven flow.

The basic steps for our FASS-CE protocol are depicted schematically in Fig. 6. These steps can be summarized as follows:

(i) Microchannel glass surface treatment: Our dynamic coating reagent, the 0.4% methylcellulose solution, was introduced into the entire chip by flowing for 30 min. All buffers used in the experiment contain the same amount of methylcellulose in an effort to keep EOF suppressed throughout the chip.

(ii) Introduction of a high-conductivity gradient region in the separation channel: A high-conductivity buffer was loaded in the separation channel reservoir (designated as east in the figure) and driven through the porous plug for about 1 min and into the chip using a computer-controlled syringe pump system. Next, a low-conductivity buffer was introduced through the injection region using pressure-driven flow from the north to the south reservoirs for about 10 s.

(iii) Sample loading: Once the high-conductivity gradient is established in the separation channel, the anionic sample was electrophoretically loaded into the double-T injector region. To this end, the south reservoir was filled with the sample mixture of Bodipy and fluorescein and electrically grounded. A 1 kV potential was then applied at the north reservoir.

(iv) Stacking and separation: Once the conductivity gradient was established and the sample loaded, a 3 kV potential was applied at the east reservoir and the west reservoir was electrically grounded, establishing an east-to-west electric field. This field initiated both sample stacking and electrophoretic separation of the negatively charged sample ions.

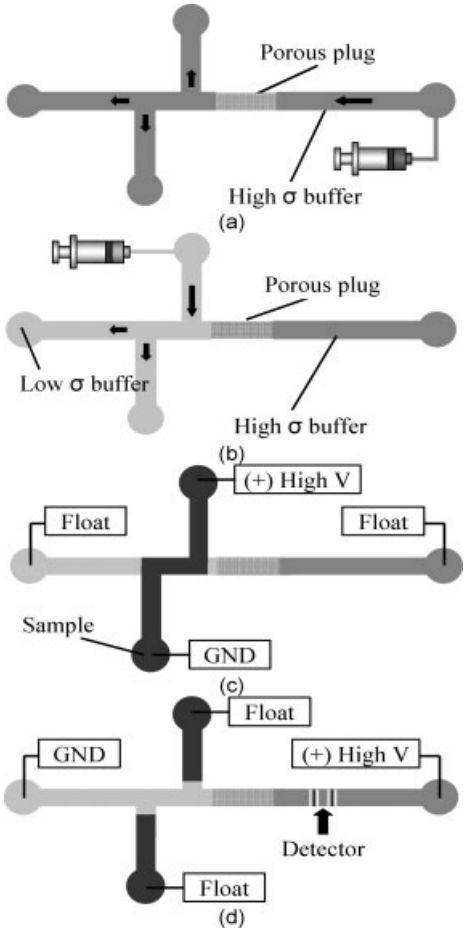

Figure 6. Schematic of FASS-CE assay protocol. (a) High-conductivity buffer is injected from the east reservoir, through the porous structure, and into all channels. This first step takes longest (about 2 min) because of the high fluidic resistance of the porous plug. Arrows show the direction of pressure-driven flow. (b) Low-conductivity buffer is introduced from the west reservoir at a flow rate of approximately 0.1 μL/min for 0.5 min. Here, the porous structure provides high fluidic-resistance which minimizes the mixing of two buffers at the upstream plug/buffer interface. (c) Sample is then electrokinetically loaded into the double-T injector. Negatively charged sample ions electromigrate from the south reservoir (grounded) to the north reservoir (1 kV). (d) Stacking, separation, and detection of samples in the separation channel. The separated sample bands are depicted in the figure as two rectangles near the detector.

(v) Sample detection: Separated sample peaks were detected using an epifluorescent microscope and CCD camera with a viewing region positioned 10 mm downstream of the injection region.

As indicated before, an important aspect of this sample injection scheme is that it avoids electrokinetic instabilities associated with high-conductivity gradient regions

near channel intersections where both conductivity gradients and electric fields are three-dimensional. During electrophoretic sample injection (Step iii, where we use an electric field to introduce sample into the injection region), the electric field in the region of high-conductivity gradients (at the left-hand edge of the porous plug) is apparently too low to induce electrokinetic instabilities. This is consistent with the work of Chen *et al.* [10] who found that electrokinetic flows with high-conductivity gradients have a critical electric field below which they are stable. During the FASS/separation step (Step iv), we hypothesize that the electrokinetic instability is still avoided because the region of high-conductivity gradient is confined to a straight-channel section (away from intersections) where the electric field is mostly parallel to the conductivity gradient.

2.5 Figures of merit in FASS

The efficiency of a FASS-CE system can be characterized as the enhancement of sample concentration for a given conductivity ratio (γ). This enhancement can be quantified in terms of either absolute sample concentration increase or signal increase. Below we present two such definitions applicable to optical detectors in terms of an observable quantity, I, which is the intensity signal measured by the detector. The first figure of merit is a concentration increase, *CI*, which can be characterized as

$$CI = \frac{I_{s,\max} - I_b}{I_0 - I_b} \quad (1)$$

where $I_{s,max}$ is the local maximum measured intensity of the stacked sample, and I_o is the original, relatively uniform measured intensity of the sample. Both of these signals are normalized by a subtraction of the background intensity of the image, I_b (the signal of the local system without sample injection). As shown schematically in Fig. 7, $I_{s,max}$ is simply the maximum of the spatially and temporally varying measured intensity signal associated with a sample band. This figure of merit can be difficult to quantify without CCD imaging as the signal value I_o occurs in the injection channel and $I_{s,max}$ occurs in a region of the channel that may not be known *a priori*. This measure is based on intensity measurements in two different regions and is of particular interest to fundamental studies of FASS dynamics [14].

A second figure of merit we can define is the ratio of the signal of stacked sample (at the point of detection of the electropherogram) to that of unstacked sample at the same point of detection. This signal increase figure, *SI*, can be expressed as

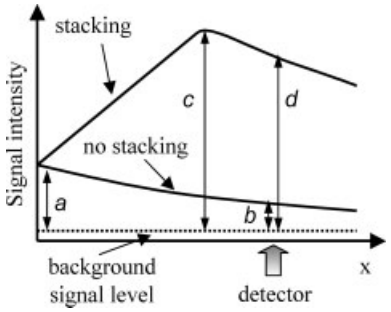

Figure 7. Schematic of signal strength as a function of downstream location along the separation channel, *x*, of a single molecular species for both a FASS separation and an unstacked separation process (denoted as "no stacking"). The intensity of the FASS signal increases as the (negatively charged) sample stacks at the rear interface of the sample buffer region. After stacking, the sample disperses (decreasing signal intensity) as it electromigrates through the high-conductivity background buffer. Four signal intensities of interest are the original, upstream sample intensity, *a*, the intensity of analyte detected by a point-wise downstream detector for "no stacking" conditions, *b*, the maximum intensity of the stacked analyte, *c*, and the intensity of the stacked analyte detected by the downstream point-wise detector, *d*. Two figures of merit are the ratios *c*/*a* and *d*/*b*, which are respectively the concentration increase, *CI*, and the signal increase, *SI*.

$$SI = \frac{I_s - I_b}{I_u - I_b} \quad (2)$$

where now I_s and I_u both occur at the desired point of detection and are associated with different experiments (one with stacked samples and one without stacking). Note that both I_s and I_u are temporal signal maxima. While *CI* gives an absolute measure of the efficiency of FASS for a single experiment, *SI* is a more easily measurable quantity of practical interest to CE system designers. In simple FASS, the theoretical limit of *CI* is the conductivity ratio, γ [14]. However, actual concentration increases obtained in practice are less than the theoretical maximum due to dispersion of sample analytes [11, 14]. *SI* can be substantially higher than *CI* provided that samples detected downstream have had significant band broadening during the post-stacking, separation process. As with any electrophoretic separation, two other important figures of merit in FASS assays are peak resolution, *R*, and the signal-to-noise ratio, *SNR*, of signal peaks. The former can be defined as the distance between peaks divided by the standard deviation width of the wider peak. *SNR* is defined as the ratio of a signal peak height above a mean noise level (*e.g.*, signal values *c* and *d* in Fig. 7) to twice the standard deviation of the background signal. The *SNR-R* model is discussed in detail by Bharadwaj *et al*. [15].

3 Results and discussion

3.1 CCD imaging calibration

During the FASS process, the concentration of sample ions changes significantly. Since the dynamic range of a CCD is limited, detection of both the dilute and stacked sample intensities is often not possible using the same imaging process. The signal of a dilute sample may be below the limit of detection, while that of a stacked sample may saturate a CCD. To accommodate drastic changes in signal strength, we adjusted exposure time of our CCD camera. Figure 8a shows the results of a calibration experiment which demonstrates that signal intensity is linearly proportional to the exposure time, Δt, over the range of interest. From this calibration, sets of data colleted using different exposure times can be normalized as $I^* = I/\Delta t$, where I is the raw intensity data minus the background level, and compared. We also calibrated the intensity of the CCD with respect to the concentration of fluorescein samples as shown in Fig. 8b. Together, these measurements suggest that measured signals are proportional to fluorophore concentrations for our samples and exposure times.

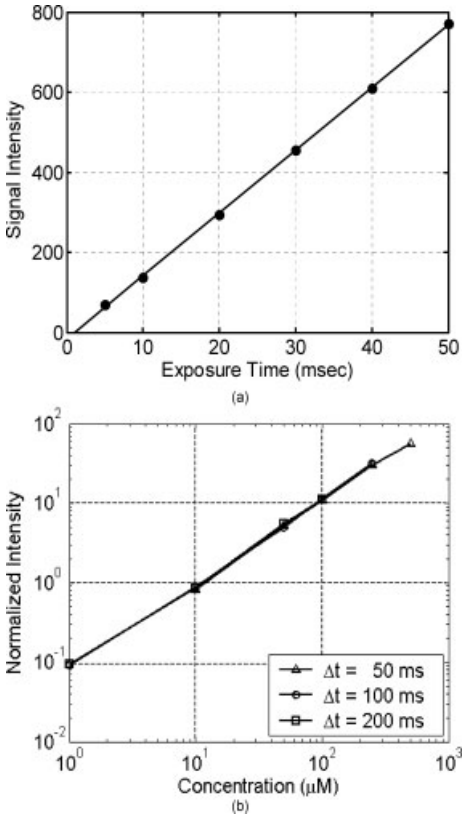

Figure 8. Calibration of the CCD imaging system for various exposure times and sample concentrations. (a) Signal intensity *versus* CCD exposure time for 1 μM fluorescein sample in a 100 by 100 μm square cross-section capillary. (b) Signal intensity *versus* concentration of fluorescein for three exposure times (the three curves are nearly indistinguishable). All image data shown here were obtained using a 10× objective with a numerical aperture of 0.3.

3.2 Sample stacking results

Figure 9 shows the initial development of an injected sample band under stacking conditions. This figure is a composite of width-averaged, axially varying intensity profiles at various times for a 1.2 mm wide region immediately downstream of the porous plug. In this experiment, we used a buffer system with $\gamma = 320$ and the sample is a 1 μM fluorescein. The concentration increase, *CI*, is about 160 at this location centered 1.8 mm downstream of the injection region, but has not reached the expected plateau within the field of view. Figure 10 shows a plug profile during the FASS process. The nearly ideal shape of this sample band demonstrates that dispersion due to internal pressure-gradients is undetectable. These gradients can be contrasted to the highly dispersed concentration profiles of systems without EOF suppression [14]. We have used this FASS-CE system to effect a separation of 2 μM and 1 μM initial concentrations of fluorescein and Bodipy, respectively. Figure 11 shows the separation of sample analytes detected at a point 10 mm downstream of the intersection of the double-T injection region. The electropherograms are determined by spatially integrating full-field CCD imaging data over a 5000 μm^2 region centered on the channel centerline to simulate the detec-

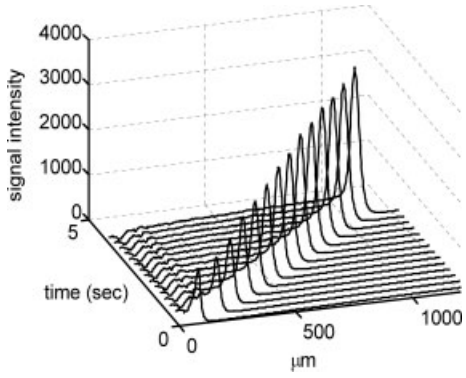

Figure 9. Plots of signal intensity *versus* axial location along the separation channel showing the development of stacking process. Each curve is a column-averaged (along the width of channel) axial intensity profile. The curves correspond to 14 CCD images of a region immediately downstream of the porous polymer structure in the chip. The conductivity ratio in this experiment is 320. The images were obtained at a 32.2 Hz frame rat using a 10× objective (NA = 0.3) and with exposure times of 20 ms.

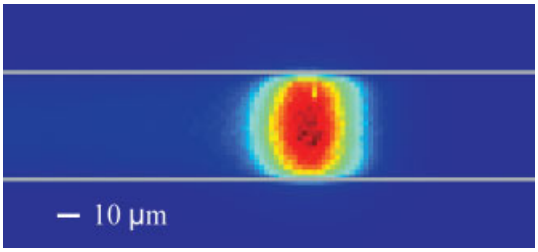

Figure 10. Image of a stacked sample band of fluorescein at a location 1.8 mm downstream from the double-T injector intersection of the chip. This image corresponds to the 12th intensity profile shown in Fig. 8 at 3.1 s (the peak is approximately at $x = 910$ µm). The white horizontal lines have been added to denote the position of microchannel walls. The nearly vertical gradients in intensity within the channel are consistent with a low dispersion separation.

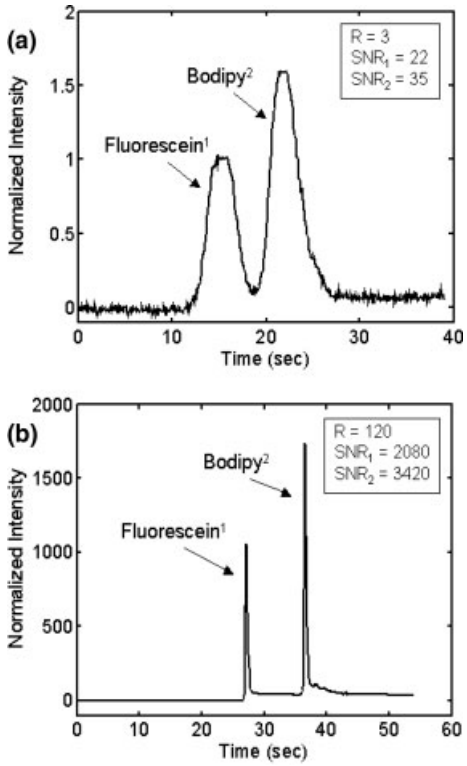

Figure 11. Electropherograms of fluorescein and Bodipy separations. Fluorescence signal is normalized with exposure time in both plots. The position of the detector is 10 mm from the downstream channel intersection of the chip. (a) Electropherogram of analytes in a CE separation and detection performed without stacking: conductivity ration, γ, of unity. Exposure time for each image is 50 ms. (b) Stacked CE electropherogram for a conductivity ration, γ, of 1290. The exposure time in this case is 5 ms. The differences in electromigration times are due to the effects of FASS. The signal increase is 1100-fold for the stacked case, and resolution increases from 3 to 120.

tion of a point-wise photodetector (*e.g.*, a photomultiplier tube) and to increase the effective sensitivity of our CCD-based detector. Figure 11a shows the results of a CE separation performed using the porous plug chip with matched sample and background buffers (*i.e.*, no stacking with $\gamma = 1$). The resolution of these peaks, *R*, is 3, and their *SNR*s are 35 and 22 for Bodipy and fluorescein, respectively. Figure 11b depicts an electropherogram detected at the same location and in the same chip with $\gamma = 1290$. This aggressive FASS process leverages a background buffer with 77.6 mS/cm conductivity and a low-conductivity (60.1 µS/cm) sample buffer. This experiment achieves a *CI* of 580. *R* is 120 and the *SNR* of the peaks are 3420 and 2080 for Bodipy and fluorescein, respectively. Comparison of the two data sets demonstrates a signal increase, *SI*, of 1100. This signal increase is a factor of 10 larger than the highest on-chip FASS signal increases previously reported [7, 8].

4 Concluding remarks

We have developed a novel CE device and separation protocol which uses a porous structure to facilitate robust, high-gradient on-chip FASS. The porous structure enables the use of a pressure-injection scheme for the introduction of a high-conductivity gradient in a separation channel and thereby avoids flow instabilities associated with high-conductivity gradient electrokinetics. This device, and its associated injection process, avoids the need for complex channel intersection geometries and/or accurate pressure- and electrokinetically driven flow control techniques (including valving). The approach also allows for the suppression of EOF and benefits from the associated minimization of sample dispersion caused by nonuniform EOF mobilities. The injection procedure used in this chip has a single pressure-flow high-conductivity buffer injection step followed by standard high-voltage control of electrophoretic fluxes of sample. A characterization of this device shows a signal increase factor of 1100, which is the highest sensitivity enhancement reported so far using on-chip FASS as a stand-alone method. The FASS experiments also demonstrate significant increases in signal-to-noise ratio and resolution. Further optimization of the porous plug characteristics, size, and location should provide higher performance and reproducible sample preconcentration CE assays.

This work is funded by DARPA grant F30602-00-2-0609 (Symbiosys program). The authors thank Drs. Jennifer Tripp and Frantisek Svec for assistance with polymer frit fabrication and pore size characterization.

Received December 17, 2002

5 References

[1] Manz, A., *Chimia* 1996, *50*, 140–143.

[2] Landers, J. P., *Handbook of Capillary Electrophoresis*, 2nd Edition, CRC Press, Boca Raton, FL 1997.

[3] Mikkers, F. E. P., Everaerts, F. M., Verheggen T., *J. Chromatogr.* 1979, *169*, 1–10.

[4] Jacobson, S. C., Ramsey, J. M., *Electrophoresis* 1995, *16*, 481–486.

[5] Beckers, J. L., Boček, P., *Electrophoresis* 2000, *21*, 2747–2767.

[6] Osbourn, D. M., Weiss, D. J., Lunte, C. E., *Electrophoresis* 2000, *21*, 2768–2779.

[7] Lichtenberg, J., Verpoorte, E., de Rooij, N. F., *Electrophoresis* 2001, *22*, 258–271.

[8] Yang, H., Chien, R. L., *J. Chromatogr. A* 2001, *924*, 155–163.

[9] Devasenathipathy, S., Bharadwaj, R., Santiago, J. G., *ASME International Mechanical Engineering Congress and Exposition* 2002, New Orleans, LA, CD Vol. 1, No. 33556.

[10] Chen, C. H., Santiago, J. G., *ASME International Mechanical Engineering Congress and Exposition* 2002, New Orleans, LA, CD Vol. 1, No. 33563.

[11] Burgi, D. S., Chien, R. L., *Anal. Chem.* 1991, *63*, 2042–2047.

[12] Herr, A. E., Mikkelsen, J. C., Santiago, J. G., Kenny, T. W., *IMECE 2000 MicroFluidics Symposium, ASME International Mechanical Engineering Congress and Exposition* 2000, Orlando, FL pp. 515–518.

[13] Yu, C., Xu, M. C., Svec, F., Fréchet, J. M. J., *J. Polymer Sci. Part A* 2002, *40*, 755–769.

[14] Bharadwaj, R., Santiago, J. G., *ASME International Mechanical Engineering Congress and Exposition, Sixth Micro-Fluidic Symposium* 2001, New York, NY, CD Vol. 2, No. 23885.

[15] Bharadwaj, R., Santiago, J. G., Mohammadi, B., *Electrophoresis* 2002, *23*, 2729–2744.